

Communication Rate Analysis for Event-based State Estimation

Simon Ebner and Sebastian Trimpe

Abstract—The average communication in a typical event-based state estimation scenario is analyzed analytically and in robot experiments. A sender observes a linear Gaussian process and sporadically transmits mean and variance to a remote estimator according to an event-based protocol. By exploiting the event-based architecture, an expression for the average communication rate is obtained, which is useful for numerical computation. In addition, approximate closed-form expressions for the steady-state rate (given in terms of problem and design parameters) are derived. The analytic results for the communication rate are verified in experiments of a one-dimensional robot link.

I. INTRODUCTION

Event-based methods for control, estimation, and optimization (see e.g. [1]–[3]) aim at achieving a better compromise between system performance and usage of system resources (e.g. processing and communication) than traditional designs. In contrast to the traditional time-based designs, data are not processed or transmitted at pre-determined times (typically, periodically at fixed rates), but only when needed to ensure a certain system-level performance. This is achieved by introducing event triggering mechanisms that decide at run time whether a controller or estimator update is necessary (e.g. when a control error grows too large or an estimate becomes too uncertain). In this way, communication and processing instants can typically be reduced significantly.

While fewer data usually corresponds to less accuracy, reducing communication may well improve performance when viewed from a system-level perspective. For example, reducing data transmissions in battery-powered wireless networks increases the lifespan of the system, or a blocked link being a bottleneck in a network might be relieved by reducing traffic. Being able to estimate the resulting communication rates is of prime interest to evaluate an event-based system design. For example, the communication rate allows one to estimate resource savings, to design system components such as link bandwidth, and – last, but not least – judge whether the increased overhead compared to traditional system design is justified.

While significant savings in data rates have been demonstrated in simulation studies (e.g. [4]–[7]) and experiments on physical platforms (e.g. [8]–[10]), there are fewer results that provide analytic expressions for the communication rate based on problem and design parameters. Obviously, such formula, even if only approximate, are helpful to support

The authors are with the Autonomous Motion Department at the Max Planck Institute for Intelligent Systems, 72076 Tübingen, Germany. simon.ebner@gmail.com, trimpe@tuebingen.mpg.de

This work was supported by the Max Planck Society and the Max Planck ETH Center for Learning Systems.

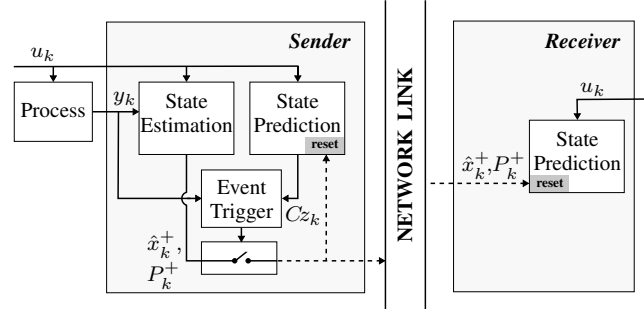


Fig. 1. High-level architecture of the considered event-based communication scheme. Event-based communication is indicated by dashed lines. The object of this paper is to derive an expression for the average communication rate from *Sender* to *Receiver*. The input u_k is assumed known on both sides, which can be achieved through another event-based link, [11].

design decisions at an early stage, or back up simulation results, for instance.

Contributions: In this paper, we analyze the communication rate for an archetypal setup for *event-based state estimation*. We consider the remote estimation scenario depicted in Fig. 1, where a smart sensor (“*Sender*”) estimates the state of a dynamic process from measurements and sporadically transmits its estimates to a remote estimator (“*Receiver*”) over a network link (details of the architecture to be discussed in Sec. II). For an assumed linear Gaussian process and typical implementations of the event trigger and estimation routines, we compute the expected communication rate; that is, we answer: *How often is a communication from Sender to Receiver triggered on average?*

Let γ_k denote the binary random variable indicating whether communication occurs ($\gamma_k = 1$) or not ($\gamma_k = 0$). In detail, we make the following contributions:

- An expression for the expected communication rate $\mathbf{E}[\gamma_k]$ is derived, which exploits the structure of the event-based architecture and allows for recursive computation via numerical integration.
- Observing that $\mathbf{E}[\gamma_k]$ converges to a steady-state value in the considered scenario, we compute the steady-state rate $\bar{\gamma} = \lim_{k \rightarrow \infty} \mathbf{E}[\gamma_k]$.
- Through Taylor series approximations of different order, we derive closed-form expressions for $\bar{\gamma}$ in terms of the process parameters and the triggering threshold.
- The analytic communication rates are compared to empirical rates obtained in experiments estimating the position and velocity of a robot link.

The architecture in Fig. 1 is adopted from [11], where it was proposed for remote operation of robots (see Sec. II

for details). The main contribution of this work is the theoretical and experimental communication rate analysis for this architecture.

Related work: For surveys of recent results in event-based state estimation, we refer the reader to [3], [12], [13] and references therein. Related work also analyzing communication rates in event-based state estimation can be found in [14]–[16], which we briefly review next.

Typically, posterior state distributions in event-based estimation are non-Gaussian, even if the process is linear Gaussian (see e.g. [7], [15], [17], [18]). This fundamental issue considerably complicates analysis of event-based estimation schemes in general, and the computation of communication rates in particular. Hence, a common approach is to approximate the conditional state distribution as actually being Gaussian to facilitate further computations. Wu et al. used this approach to compute approximate communication rates for a scenario similar to the one herein [14]. In contrast, we do not approximate the posterior as being Gaussian, but arrive at an expression for the communication rate by exploiting the communication architecture (in particular, the fact that the posterior *after* a communication is Gaussian). In a second step, to obtain closed-form expressions in terms of the problem parameters, we employ Taylor series approximations, which can be customized to a desired order.

Instead of computing the expected communication rate directly, Shi et al. provide lower and upper bounds on it by employing ellipsoidal approximations to the triggering set, [15]. Han et al. used a different trigger mechanism altogether, [16]. By means of stochastic triggering, the probability distributions become tractable (i.e. Gaussian), which simplifies analysis such as of communication rates, but relinquishes guaranteed bounds on the prediction error.

Notation: In the following, k is used as a general time index, and s_k denotes the signal s evaluated at index k . We use $s_{k:k+L}$ with $L \geq 0$ to denote the concatenation of the vectors $s_k, s_{k+1}, \dots, s_{k+L}$ into one long vector.

For discrete random variables (RVs) x and y , we write $p(x)$ and $p(x|y)$ for the probability and conditional probability. For continuous RVs x and y , $f(x)$ and $f(x|y)$ denote the (conditional) probability density functions (PDF). We use the notation $(x|y)$ to refer to the random variable x conditioned on y , and $\mathbf{E}[\cdot|y]$ is the conditional mean.

For a symmetric, positive definite matrix A , $A^{\frac{1}{2}}$ denotes the Cholesky decomposition of A such that $(A^{\frac{1}{2}})^T A^{\frac{1}{2}} = A$.

II. EVENT-BASED STATE ESTIMATION ARCHITECTURE

This section introduces the components of the remote estimation problem and the event-based architecture as shown in Fig. 1. This event-based architecture has been applied in [11] for remote operation of a robot. In this example, the robot estimates a state x_k (e.g. including its own state and the state of the environment) from measurements y_k , and transmits its estimates, such as posterior mean \hat{x}_k^+ and variance P_k^+ , to an operator for the purpose of monitoring, for example. Communication occurs according to an event-based protocol ensuring that data is transferred only when necessary. Thus,

the robot constitutes the *sender* in Fig. 1, and the operator corresponds to the *receiver*. The framework in [11] proposes an event-based protocol also for the link from operator to robot, which is used to transmit control inputs or policies. This ensures that the current input u_k is known on both sides, which is also assumed herein (cf. Fig. 1). This work focuses on the robot-to-operator only as shown in Fig. 1. Moreover, we consider the special case of a linear Gaussian process. While motivated from the remote robot operation problem in [11], the considered architecture is not specific to this problem and applies to other remote estimation scenarios likewise.

The key idea of the event-based architecture is to implement a state predictor on both sides, the sender and the receiver. On the receiver side, the state predictor makes predictions of the state to compensate for times when no up-to-date estimation data is communicated. The sender implements a copy of the same state prediction and compares this to the current estimates in order to decide when new data should be triggered. In the next subsections, all blocks of Fig. 1 are introduced.

A. Process model

We consider the linear, discrete-time process model

$$\begin{aligned} x_{k+1} &= Ax_k + Bu_k + v_k \\ y_k &= Cx_k + w_k \end{aligned} \quad (1)$$

with state $x_k \in \mathbb{R}^n$, control input u_k , observation $y_k \in \mathbb{R}^m$, and zero-mean, Gaussian distributed noise v_k and w_k with covariances $Q \geq 0$ and $R > 0$. We assume that (A, C) and (A, G) are detectable and stabilizable, respectively, where $Q = G^T G$. The initial state x_0 is Gaussian with zero mean and covariance $P_0^x > 0$. In this work, we focus on the pure state estimation problem and assume that the input u_k is known to both the receiver and the sender (cf. Fig. 1). Furthermore, the model parameters of (1) are assumed known.

B. State estimation

The sender has periodic access to all measurements $Y_k := \{y_0, \dots, y_k\}$, from which it estimates the system state x_k (State Estimation in Fig. 1). From standard filtering theory [19], the conditional state $(x_k|Y_k)$ is known to be Gaussian distributed, and the optimal Bayesian estimator is the discrete-time Kalman filter, which recursively computes mean and variance:

$$\begin{aligned} \hat{x}_k^- &= \mathbf{E}[x_k|Y_{k-1}] & P_k^- &= \mathbf{E}[(x_k - \hat{x}_k^-)(x_k - \hat{x}_k^-)^T | Y_{k-1}] \\ \hat{x}_k^+ &= \mathbf{E}[x_k|Y_k] & P_k^+ &= \mathbf{E}[(x_k - \hat{x}_k^+)(x_k - \hat{x}_k^+)^T | Y_k]. \end{aligned}$$

The recursive update equations can be found in [19], for example.

C. State prediction

The state prediction on sender and receiver (see Figure 1), maintains an estimate z_k of the state x_k , which is predicted using the process model (1) at times of no communication,

and reset with the Kalman filter estimate \hat{x}_k^+ when a communication is triggered. That is,

$$z_k = \begin{cases} \hat{x}_k^+ & \text{if } \gamma_k = 1 \\ z_k^- & \text{if } \gamma_k = 0 \end{cases} \quad (2)$$

where $z_k^- := Az_{k-1} + Bu_{k-1}$, and the binary variable γ_k indicates whether a communication was triggered ($\gamma_k = 1$) or not ($\gamma_k = 0$). The event triggering mechanism will be specified in the next subsection.

In the later analysis, ℓ_k will be used to denote the most recent time when the predictor was updated, i.e.

$$\ell_k := \max\{i \leq k \mid \gamma_i = 1\}. \quad (3)$$

We will drop the argument k and usually write ℓ instead of ℓ_k when k is clear from context. The information set that the receiver (and thus the state predictor) has available at time k is given by¹

$$\mathbf{I}_k = \{y_0, \dots, y_\ell\} \cup \{\gamma_0, \dots, \gamma_k\}. \quad (4)$$

Since the Kalman filter in Sec. II-B keeps track of the entire posterior distribution $f(x_k | Y_k)$ through mean \hat{x}_k^+ and variance P_k^+ , communicating mean and variance is sufficient to synchronize the conditional state information at sender and receiver; that is,

$$f(x_k | \mathbf{I}_k) = f(x_k | Y_k) \quad \text{for } \gamma_k = 1. \quad (5)$$

D. Event trigger

The event trigger decides whether or not the conditional state PDF $f(x_k | Y_k)$ (here encoded in mean \hat{x}_k^+ and variance P_k^+) is transmitted to the receiver (Fig. 1). Different triggering mechanisms are conceivable; herein, we place a threshold on the difference between the current measurement and the prediction of the measurement

$$e_k := y_k - Cz_k^- \quad (6)$$

which can be rewritten as $e_k = C\epsilon_k + w_k$ with the state prediction error

$$\epsilon_k := x_k - z_k^-. \quad (7)$$

The event trigger is then given by

$$\gamma_k = \begin{cases} 1 & \text{if } \|e_k\|_\infty \geq \delta \\ 0 & \text{otherwise.} \end{cases} \quad (8)$$

Triggers based on the measurement prediction error (6) are known as *measurement-based* or *innovation-based triggers* and have been found to be effective triggers for state estimation, [5], [7].

We use χ to define the set of values $e \in \mathbb{R}^m$ that do not cause communication using the trigger (8)

$$\chi := \{e \in \mathbb{R}^m \mid \|e\|_\infty < \delta\}. \quad (9)$$

¹We remark that the state predictor (2) does not exploit the information that is contained in the events, where no communication happens (i.e. $\gamma_k = 0$ for $k > \ell_k$). Conditioning on the information $\gamma_k = 0$ typically yields significantly more involved filtering algorithms. See discussion in [7], for example.

III. PROBLEM FORMULATION

The object of this paper is to obtain an expression for the expected communication rate $\mathbf{E}[\gamma_k]$. In principle, we can compute the expected communication rate from the probability density function (PDF) of the error (6)

$$\mathbf{E}[\gamma_k] = 1 - p(\gamma_k = 0) = 1 - \int_{\chi} f(e_k) de_k. \quad (10)$$

Unfortunately, one cannot easily express the density $f(e_k)$ in general since z_k depends on the communication history. However, we can exploit the event-based communication scheme introduced in the previous section to facilitate the communication rate analysis. In particular, we shall use the fact that the error following an event is normally distributed. Indeed, if a communication is triggered at time k ($\gamma_k = 1$), $f(x_k | \mathbf{I}_k)$ is Gaussian (see (5)), and likewise the distribution of the error $p(e_{k+1} | \mathbf{I}_k)$, as well as future predicted errors $p(e_{k+L}, \dots, e_{k+1} | \mathbf{I}_k)$, $L \geq 1$. This observation will be used to efficiently compute the communication rate.

The next section formally establishes the above result, which is then used in Sec. V to derive an expression for $\mathbf{E}[\gamma_k]$, which can be used for numerical integration. Furthermore, we address the steady-state communication rate and provide (based on Taylor-series approximations of different orders) closed-form expressions that allow to compute the steady-state rate directly from the problem parameters A , C , Q , R , and δ .

IV. PRELIMINARIES

The following lemma establishes that the multivariate distribution of all state prediction errors (6) for all times following after a communication event, i.e. $k > \ell_k$, is Gaussian.

Lemma 1: The joint PDF $f(\epsilon_{\ell+1:\ell+L} | \mathbf{I}_\ell) = f(\epsilon_{\ell+1}, \dots, \epsilon_{\ell+L} | \mathbf{I}_\ell)$, $L \geq 1$ is described by a multivariate Gaussian distribution with zero mean and covariance $\Phi_{\ell+1:\ell+L}$. $\Phi_{\ell+1:\ell+L}$ consists of $L \times L$ blocks where the (i, j) block is given by

$$A^i P_\ell^+ (A^j)^\top + \sum_{k=1}^i A^{i-k} Q (A^{j-k})^\top \quad (11)$$

for $j \geq i \geq 1$ and $i > j \geq 1$ follows from symmetry.

Proof: Let $\Delta_\ell := (x_\ell - \hat{x}_\ell^+ | \mathbf{I}_\ell)$. Because of the communication at ℓ , we have $(x_\ell - \hat{x}_\ell^+ | \mathbf{I}_\ell) \equiv (x_\ell - \hat{x}_\ell^+ | Y_\ell)$; that is, the estimation errors at sender and receiver have the same distribution. Hence, Δ_ℓ is Gaussian distributed with zero mean and covariance P_ℓ^+ (see e.g. [20]). For the prediction error (7), it follows that

$$\begin{aligned} (\epsilon_{\ell+1} | \mathbf{I}_\ell) &= (x_{\ell+1} - z_{\ell+1}^- | \mathbf{I}_\ell) \\ &= (Ax_\ell - Az_\ell + v_\ell | \mathbf{I}_\ell) \\ &= A(x_\ell - \hat{x}_\ell^+ | \mathbf{I}_\ell) + (v_\ell | \mathbf{I}_\ell) \\ &= A\Delta_\ell + v_\ell \end{aligned} \quad (12)$$

$$\begin{aligned} (\epsilon_{\ell+2} | \mathbf{I}_\ell) &= A^2\Delta_\ell + Av_\ell + v_{\ell+1} \\ &\vdots \\ (\epsilon_{\ell+i} | \mathbf{I}_\ell) &= A^i\Delta_\ell + \sum_{k=1}^i A^{i-k} v_{\ell+k-1} \end{aligned}$$

and hence,

$$\begin{pmatrix} \epsilon_{\ell+1} \\ \epsilon_{\ell+2} \\ \vdots \\ \epsilon_{\ell+i} \end{pmatrix} \Big| \mathbb{I}_\ell = \begin{bmatrix} A \\ A^2 \\ \vdots \\ A^{i\ell} \end{bmatrix} \Delta_\ell + \begin{bmatrix} I & \cdots & 0 \\ A & I & \cdots & 0 \\ \vdots & & \ddots & \\ A^{i-1}A^{i-2} & \cdots & I \end{bmatrix} \begin{bmatrix} v_\ell \\ v_{\ell+1} \\ \vdots \\ v_{\ell+i-1} \end{bmatrix}$$

Since Δ_ℓ and v_k for all $k > \ell$ are independent, the Gaussian property is immediate [21], and mean and variance follow from the above expression. ■

From (1), (6), and (7), we have $e_k = C\epsilon_k + w_k$. Thus, the Gaussian property of e_k follows directly from Lemma 1 and independence of w_k .

Lemma 2: The joint PDF $f(e_{\ell+1:\ell+L} | \mathbb{I}_\ell) = f(e_{\ell+1}, \dots, e_{\ell+L} | \mathbb{I}_\ell)$, $L \geq 1$ is a multivariate Gaussian with zero mean and covariance

$$\Sigma_{\ell+1:\ell+L} = (\mathbb{I}_L \otimes C) \Phi_{\ell+1:\ell+L} (\mathbb{I}_L \otimes C^T) + \mathbb{I}_L \otimes R \quad (13)$$

where $\mathbb{I}_L \in \mathbb{R}^{L \times L}$ denotes the identity matrix and $A \otimes B$ is used to denote the Kronecker product of A and B .

V. COMMUNICATION RATE ANALYSIS

The expected communication rate $\mathbf{E}[\gamma_k] = p(\gamma_k = 1)$ can be expressed generically by marginalizing the joint probability $p(\gamma_k, \dots, \gamma_0)$ over the past communication decisions γ_i , $i < k$:

$$\begin{aligned} \mathbf{E}[\gamma_k] &= p(\gamma_k = 1) = 1 - p(\gamma_k = 0) \\ &= 1 - p(\gamma_k = 0, \gamma_{k-1} = 0) - p(\gamma_k = 0, \gamma_{k-1} = 1) \\ &\quad \vdots \\ &= 1 - \sum_{\substack{\Gamma_i \in \{0,1\} \\ i=0, \dots, k-1}} p(\gamma_k = 0, \gamma_{k-1} = \Gamma_{k-1}, \dots, \gamma_0 = \Gamma_0). \quad (14) \end{aligned}$$

The summation in (14) involves all 2^k combinations; that is, computation grows exponentially. We can reduce the number of summands from 2^k to k using the result from Sec. IV. Lemma 2 states that the joint PDF of the triggering signals $e_{\ell+1}, \dots, e_{\ell+L}$ following a communication event at time ℓ are Gaussian and known. Hence, also the probability of not communicating consecutively L times in a row after a communication at time ℓ , i.e. $p(\gamma_{\ell+L} = 0, \dots, \gamma_{\ell+1} = 0 | \gamma_\ell = 1)$, can be computed. Therefore, the branches in equation (14) do not need to be expanded beyond a communication event $\gamma_i = 1$. Setting $p_0 := p(\gamma_k = 0, \dots, \gamma_0 = 0)$ we thus obtain

$$\begin{aligned} \mathbf{E}[\gamma_k] &= p(\gamma_k = 1) \\ &= 1 - \sum_{i=0}^{k-1} p(\gamma_k = 0, \dots, \gamma_{i+1} = 0, \gamma_i = 1) - p_0 \\ &= 1 - \sum_{i=0}^{k-1} p(\gamma_k = 0, \dots, \gamma_{i+1} = 0 | \gamma_i = 1) p(\gamma_i = 1) - p_0 \\ &= 1 - \sum_{i=0}^{k-1} \int_{\chi^{k-i}} f(e_{i+1:k} | \gamma_i = 1) de_{i+1:k} p(\gamma_i = 1) - p_0 \quad (15) \end{aligned}$$

where we introduced the set notation

$$\chi^d := \underbrace{\chi \times \chi \cdots \times \chi}_{d\text{-times}} \quad (16)$$

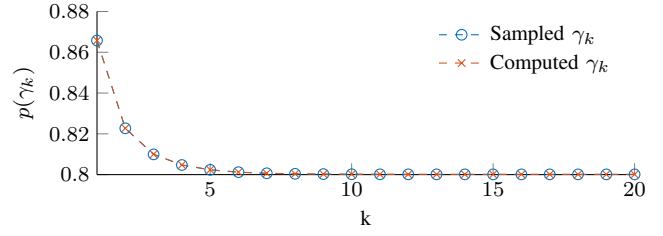


Fig. 2. Evolution of the communication rate γ_k for the scalar system in Example 5.1. Blue: Monte Carlo simulation. Red: computed from (15) by numerical integration.

with χ as in (9) to denote the integration set. From Lemma 2, we have that $f(e_{i+1:k} | \gamma_i = 1)$ is Gaussian with zero mean and variance $\Sigma_{i+1:k}$, which can be computed from (13). Equation (15) can be used to compute the average communication rate recursively because $\mathbf{E}[\gamma_k]$ depends on the previous $p(\gamma_i) = \mathbf{E}[\gamma_i]$, $i = 1, \dots, k-1$. Each iteration requires the integration of a multivariate Gaussian.

Example 5.1: For a scalar linear system (1) with $A = 1.1$, $C = 1$, $Q = 0.05$, $R = 0.1$, $P_0^x = 1.0$, and $\delta = 0.15$, the average communication rate $\mathbf{E}[\gamma_k]$ is shown for the first 20 time steps in Fig. 2. The example compares the communication rate computed by numerical integration of (15) (red) with the communication rate obtained from Monte Carlo simulation (blue). The sampled communication rate was obtained based on 5×10^8 iterations. The Cuba framework [22] was used for the multi-dimensional integration in (15).

A. Stationary average communication rate

In the example in Fig. 2, we see that the average communication rate quickly converges to a stationary value after a few steps, which corresponds to the typical behavior also observed in other numerical simulations. Assuming that indeed the communication rate converges to a stationary value, $\bar{\gamma} = \lim_{k \rightarrow \infty} \mathbf{E}[\gamma_k]$, we derive an expression for the stationary rate $\bar{\gamma}$ from the problem data (system model and communication threshold) in this and the following subsections.

The stationary communication rate is particularly interesting when designing an event-driven system, as it directly relates to the average use of communication and processing resources, which translate to energy cost, bandwidth use, etc. For example, network capacity and bandwidth can be optimized based on these stationary rates.

Before we turn to the analysis of the stationary average communication rate, we establish some assumptions. The main assumption is that the average communication rate indeed converges:

Assumption 1: The triggering probability $p(\gamma_k = 1) = \mathbf{E}[\gamma_k]$ converges to a steady-state value; that is, there exists $\bar{\gamma} \in \mathbb{R}$ such that $\lim_{k \rightarrow \infty} \mathbf{E}[\gamma_k] = \bar{\gamma}$.

Based on all numerical simulations we have done, we conjecture that this assumption actually holds true in general (under the assumptions of a time-invariant system, stationary noise, detectability and stabilizability property as in Sec. II-A).

However, rigorously establishing this convergence is beyond the scope of this paper and deferred to future work.

From the detectability and stabilizability assumptions on the system (1), the variance P_k^+ of the Kalman filter running on the sender side (Sec. II-B) is known to converge to the unique positive definite solution P_s to the discrete-time Riccati equation (see e.g. [19])

$$AP_sA^T - P_s - AP_sC^T(CP_sC^T + R)^{-1}CP_sA^T + Q = 0.$$

For the following analysis, we shall assume that the Kalman filter on the sender side has converged:

Assumption 2: $P_k^+ = P_s$ for all k .

From Lemma 2 with Assumption 2, it follows that

$$\begin{aligned} p(\gamma_{k+n} = 0, \dots, \gamma_{k+1} = 0 | \gamma_k = 1) = \\ p(\gamma_{j+n} = 0, \dots, \gamma_{j+1} = 0 | \gamma_j = 1) \forall n, k, j \in \mathbb{N}. \end{aligned} \quad (17)$$

That is, $p(\gamma_{k+L} = 0, \dots, \gamma_{k+1} = 0 | \gamma_k = 1)$, $L \geq 1$ only depends on the length L but not on time k . To facilitate the notation, we introduce

$$\mathcal{P}_L := p(\gamma_L = 0, \dots, \gamma_1 = 0 | \gamma_0 = 1), L \geq 1. \quad (18)$$

Using Assumption 2 and (18), we rewrite (15) as

$$\mathbf{E}[\gamma_k] = p(\gamma_k = 1) = 1 - \sum_{i=0}^{k-1} \mathcal{P}_{k-i} p(\gamma_i = 1) - p_0. \quad (19)$$

From this, and equipped with the above assumptions, we have the following result for $\bar{\gamma} = \lim_{k \rightarrow \infty} p(\gamma_k = 1) = \lim_{k \rightarrow \infty} \mathbf{E}[\gamma_k]$.

Theorem 1: Under Assumptions 1 and 2, the stationary communication rate is

$$\bar{\gamma} = (1 + \mathcal{S})^{-1} \quad (20)$$

with $\mathcal{S} := \sum_{k=1}^{\infty} \mathcal{P}_k$.

Proof: We shall show that $\bar{\gamma} = 1 - \sum_{i=1}^{\infty} \mathcal{P}_i \bar{\gamma}$ from which the original statement follows trivially. We show this by proving

$$\forall \epsilon > 0 \exists N = N(\epsilon) : \forall k > N, \left| 1 - \sum_{i=1}^k \mathcal{P}_i \bar{\gamma} - \bar{\gamma} \right| < \epsilon. \quad (21)$$

From (29), we have that $\mathcal{P}_k < \mathcal{Z}^k$. With the same reasoning, we see that $p_0 := p(\gamma_k = 0, \dots, \gamma_0 = 0) \leq \mathcal{Z}^{k+1}$. By Assumption 1, the limit of $p(\gamma_k = 1)$ for $k \rightarrow \infty$ exists; therefore,

$$\forall \epsilon_\gamma > 0 \exists N_\gamma = N_\gamma(\epsilon_\gamma) : \forall k > N_\gamma, |p(\gamma_k = 1) - \bar{\gamma}| < \epsilon_\gamma.$$

We set $\epsilon_\gamma := \frac{1}{4}\epsilon(1 - \mathcal{Z})$, and define $\epsilon_i := \bar{\gamma} - p(\gamma_i = 1)$, for which holds that $|\epsilon_i| < \epsilon_\gamma$ for $i > N_\gamma$. Also, we define $\bar{\epsilon}$ as the maximum absolute value over the finite set of ϵ_i , $i \leq N_\gamma$, i.e. $\bar{\epsilon} := \max\{|\epsilon_0|, |\epsilon_1|, \dots, |\epsilon_{N_\gamma}|\}$.

Rewriting the expression in (21) yields

$$\begin{aligned} & \left| 1 - \sum_{i=1}^k \mathcal{P}_i \bar{\gamma} - \bar{\gamma} \right| \\ &= \left| 1 - \sum_{i=1}^k \mathcal{P}_i (p(\gamma_{k-i} = 1) + \epsilon_{k-i}) - p_0 + p_0 - \bar{\gamma} \right| \\ &\leq \left| 1 - \sum_{i=0}^{k-1} \mathcal{P}_{k-i} p(\gamma_i = 1) - p_0 - \bar{\gamma} \right| + |p_0| \\ &\quad + \left| \sum_{i=1}^{k-N_\gamma-1} \mathcal{P}_i \epsilon_{k-i} \right| + \left| \sum_{i=k-N_\gamma}^k \mathcal{P}_i \epsilon_{k-i} \right|. \end{aligned} \quad (22)$$

Next, we bound each of the four summands in (22) for sufficiently large k . For the first term, we can use (19),

$$\begin{aligned} & \left| 1 - \sum_{i=0}^{k-1} \mathcal{P}_{k-i} p(\gamma_i = 1) - p_0 - \bar{\gamma} \right| \\ &= |p(\gamma_k = 1) - \bar{\gamma}| < \epsilon_\gamma < \frac{1}{4}\epsilon \end{aligned} \quad (23)$$

which holds for $k > N_1 := N_\gamma$. For the second term, we use $p_0 \leq \mathcal{Z}^k$. The condition $\mathcal{Z}^k < \frac{1}{4}\epsilon$ is satisfied trivially for $\mathcal{Z} = 0$. For $\mathcal{Z} > 0$, the statement holds for all $k > N_2$ with $N_2 := \log(\frac{1}{4}\epsilon) / \log(\mathcal{Z})$. For the third term in (22), we use the fact that $|\epsilon_i| < \epsilon_\gamma$ for $i > N_1 = N_\gamma$,

$$\begin{aligned} & \left| \sum_{i=1}^{k-N_\gamma-1} \mathcal{P}_i \epsilon_{k-i} \right| \leq \sum_{i=1}^{k-N_\gamma-1} \mathcal{P}_i |\epsilon_{k-i}| \leq \epsilon_\gamma \sum_{i=1}^{k-N_\gamma-1} \mathcal{P}_i \\ &\leq \epsilon_\gamma \sum_{i=1}^{k-N_\gamma-1} \mathcal{Z}^i \leq \epsilon_\gamma \frac{1}{1 - \mathcal{Z}} = \frac{1}{4}\epsilon. \end{aligned} \quad (24)$$

Finally, for the fourth term, we can use $\bar{\epsilon}$ as defined above to obtain

$$\begin{aligned} & \left| \sum_{i=k-N_\gamma}^k \mathcal{P}_i \epsilon_{k-i} \right| \leq \sum_{i=k-N_\gamma}^k \mathcal{P}_i |\epsilon_{k-i}| \\ &\leq \bar{\epsilon} \sum_{i=k-N_\gamma}^k \mathcal{P}_i \leq \bar{\epsilon} \mathcal{Z}^{k-N_\gamma} \sum_{i=0}^{N_\gamma} \mathcal{Z}^i \\ &\leq \bar{\epsilon} \mathcal{Z}^{k-N_\gamma} \frac{1}{1 - \mathcal{Z}}. \end{aligned} \quad (25)$$

Since $\mathcal{Z} < 1$, one can find N_3 such that (25) is bounded by $\frac{1}{4}\epsilon$ for any $k \geq N_3$. The statement is trivially satisfied for $\mathcal{Z} = 0$. For $\mathcal{Z} > 0$, such N_3 is given by

$$N_3 = \frac{\log(\frac{1}{4}\epsilon) - \log \bar{\epsilon} + \log(1 - \mathcal{Z})}{\log \mathcal{Z}} + N_\gamma \quad (26)$$

In conclusion, we can set $N = \max\{N_1, N_2, N_3\}$, and (21) follows from (22) and the previously established bounds. ■

While Theorem 1 provides a closed-form expression for the sought stationary average communication rate $\bar{\gamma}$, it is impractical for direct computation as it involves the infinite sum over the probabilities $\mathcal{P}_k = p(\gamma_k = 0, \dots, \gamma_1 = 0 | \gamma_0 = 1)$. We next address approximations of \mathcal{P}_k that shall yield an expression for the communication rate in terms of the problem parameters.

B. Approximations

The probability density \mathcal{P}_k characterizes the probability of not communicating for k consecutive time steps after communicating at time 0. It can be computed by evaluating an mk -dimensional integral

$$\begin{aligned} \mathcal{P}_k &= p(|e_k| < \delta, \dots, |e_1| < \delta | \gamma_0 = 1) \\ &= \int_{\chi^k} f(e_{1:k} | \gamma_0 = 1) de_{1:k} \\ &= Z_0^k \int_{\chi^k} \exp\left(-\frac{1}{2} e_{1:k}^T \Lambda_{1:k} e_{1:k}\right) de_{1:k} \end{aligned} \quad (27)$$

where $\Lambda_{1:k} = \Sigma_{1:k}^{-1}$ is the precision, and Z_0^k denotes the normalization factor of the normal distribution with

$$Z_0 = (2\pi | (CP_s C^T + R)^{\frac{1}{2}} |)^{-\frac{1}{2}}. \quad (28)$$

The derivation of the normalization factor is given in [23]. From (27), we can find an upper bound for \mathcal{P}_k by

$$\mathcal{P}_k \leq Z_0^k \int_{\chi^k} 1 de_{1:k} = Z_0^k (2\delta)^{mk} = \mathcal{Z}^k \quad (29)$$

where we introduced $\mathcal{Z} := (2\delta)^m Z_0$.

In the following derivations, we assume the tuning parameter δ to satisfy the following constraint.

Assumption 3: $\mathcal{Z} = (2\delta)^m Z_0 < 1$.

Assumption 3 is required to rigorously establish the mathematical details below. However, we found that the obtained communication rates often also hold approximately even if Assumption 3 is violated (see later discussion in Sec. VI).

Since the integral of the normal distribution over the hypercube χ^k cannot be computed analytically, we approximate it by means of a Taylor series expansion for the exponential function, of which we shall consider a finite number of terms in the following. We thus obtain from (27)

$$\begin{aligned} \mathcal{P}_k &= Z_0^k \int_{\chi^k} \exp\left(-\frac{1}{2} \sum_{(i,j) \in \mathcal{I}(k)} e_i^T \Lambda_{i,j} e_j\right) de_{1:k} \\ &= Z_0^k \int_{\chi^k} \sum_{l=0}^{\infty} \frac{1}{l!} \left(-\frac{1}{2} \sum_{(i,j) \in \mathcal{I}(k)} e_i^T \Lambda_{i,j} e_j\right)^l de_{1:k} \end{aligned} \quad (30)$$

where $\mathcal{I}(k) := \{1, \dots, k\} \times \{1, \dots, k\}$ is the index set of all possible combinations of pairs e_i and e_j , and $\Lambda_{i,j}$ denotes the (i, j) -block of $\Lambda_{1:k}$ when partitioned into $k \times k$ blocks of size $m \times m$. We use $\tilde{\mathcal{P}}_k^N$ to denote an approximation to \mathcal{P}_k in which only the first $L + 1$ terms in (30) are kept

$$\tilde{\mathcal{P}}_k^N := Z_0^k \int_{\chi^k} \sum_{l=0}^N \frac{1}{l!} \left(-\frac{1}{2} \sum_{(i,j) \in \mathcal{I}(k)} e_i^T \Lambda_{i,j} e_j\right)^l de_{1:k}. \quad (31)$$

C. Zero-order approximation

We first consider the zero-order approximation $\tilde{\mathcal{P}}_k^0$ to \mathcal{P}_k ,

$$\tilde{\mathcal{P}}_k^0 = Z_0^k \int_{\chi^k} 1 de_{1:k} = Z_0^k (2\delta)^{mk} = \mathcal{Z}^k. \quad (32)$$

Using the approximation $\mathcal{P}_k \approx \tilde{\mathcal{P}}_k^0$ in Theorem 1, leads to the geometric series

$$\bar{\gamma}^{-1} = 1 + \mathcal{S} = 1 + \sum_{k=1}^{\infty} \mathcal{Z}^k = (1 - \mathcal{Z})^{-1}. \quad (33)$$

Under Assumption 3, we can solve the geometric series to yield a closed form solution for $\bar{\gamma}$. Thus, we obtain approximate communication rate

$$\bar{\gamma} = 1 - \mathcal{Z} = 1 - (2\delta)^m Z_0 \quad (34)$$

which holds for small δ satisfying Assumption 3, and with Z_0 as in (28). In Sec. VI, we investigate how well this approximation holds in practice for a robotic system.

D. Higher-order approximations

Following the previous procedure, also higher-order approximations can be obtained. We cannot give the full expressions due to space constraints, but we provide an outline here, how such higher-order approximations can be obtained.

First, we approximate the Taylor series in (30) by a finite sum with $N + 1$ terms; that is, we approximate $\mathcal{P}_k \approx \tilde{\mathcal{P}}_k^N$. As the accuracy of the series approximation generally increases with higher-order terms, also $\tilde{\mathcal{P}}_k^N$ will improve for larger N .

Furthermore, we approximate the infinite sum in (20) by a finite sum of length M ; that is, $\mathcal{S} = \sum_{i=1}^{\infty} \mathcal{P}_i \approx \sum_{i=1}^M \mathcal{P}_i$. Since \mathcal{P}_i is bounded by \mathcal{Z}^i with $\mathcal{Z} < 1$ by Assumption 3, the impact of missing terms \mathcal{P}_i for $i > M$ decays exponentially.

Combining both approximation, we obtain the approximation

$$\mathcal{S} = \sum_{i=1}^{\infty} \mathcal{P}_i \approx \sum_{i=1}^M \tilde{\mathcal{P}}_i^N =: \tilde{\mathcal{S}} \quad (35)$$

which yields the approximate communication rate by (20).

Ideally, we would like to have a closed-form expression for the approximation $\tilde{\mathcal{S}}$ in (35). As $\tilde{\mathcal{P}}_k^N$ depends on the precision $\Lambda_{1:k}$, finding a closed-form expression for the elements of the precision is essential. Even though the elements of the covariance $\Sigma_{1:k}$ can be expressed in terms of the system parameters (13), obtaining an expression for the inverse is not straightforward. Using Assumption 1, however, it is indeed possible to find a closed-form expression for $\Lambda_{1:k}$ in terms of the system parameters (see [23]).

VI. ROBOT EXPERIMENTS

This section presents experimental results of applying the event-based framework (Fig. 1) to estimating the angular position and velocity of a one-dimensional robot link. In particular, we compare the communication rates derived in Sec. V to the empirical rates in order to evaluate how well the theoretical analysis and assumptions hold in practice.

A. Robot model

The experiment is performed on a rotatory wrist joint of a KUKA lightweight robot LWR2. The idealized linear system dynamics in continuous time can be described in state space representation as

$$\dot{x} = A_c x + B_c \tau \quad (36)$$

with

$$x = \begin{bmatrix} \theta \\ \dot{\theta} \end{bmatrix}, A_c = \begin{bmatrix} 0 & 1 \\ 0 & -\frac{d}{I} \end{bmatrix}, B_c = \begin{bmatrix} 0 \\ \frac{1}{I} \end{bmatrix}. \quad (37)$$

where $d = 0.2114 \text{ kg m}^2/\text{s}$, $I = 0.1641 \text{ kg m}^2$. A discrete-time version (1) is obtained by exact discretization with sampling time $\Delta t = 0.001 \text{ s}$ and assuming zero-order hold at the input. Obviously, the linear model (36) is an approximation of the true robot dynamics, which, for instance, also involve nonlinear friction.

B. Identification of model parameters

The parameters of the dynamics model (36), as well as process and measurement noise are identified from data.

Dynamics: We perform a straightforward closed-loop identification procedure to obtain the dynamics parameters I and d . A sine trajectory with a frequency of $f = 0.24 \text{ Hz}$ is applied as desired trajectory θ_k^{des} on the robot joint. The robot uses an internal PID controller to produce torques τ_k for tracking θ_k^{des} . During the identification phase, the torques produced by the controller τ_k and the angular position θ_k of the robot are recorded. From the angular position, the corresponding velocity and acceleration are recovered by numerical differentiation and noncausal low-pass filtering. The time series $\tau_k, \theta_k, \dot{\theta}_k$ and $\ddot{\theta}_k$ are used to determine the parameters for (36) using least-squares regression.

Measurement noise R : The angular position θ_k is measured by a digital encoder, and we consider the encoder quantization as measurement noise. The quantization level $\Delta = 1.73 \times 10^{-6} \text{ rad}$ is determined from a sensor readings at standstill. Assuming a uniform distribution over the quantization interval $[-\frac{\Delta}{2}, \frac{\Delta}{2}]$, the variance of the sensor noise is computed as $R = \frac{1}{12} \Delta^2 = 2.49 \times 10^{-13}$.

Process noise Q : The process noise v_k is used to describe the uncertainty that is not explained by the robot model (1). Solving for v_k yields

$$v_k = x_{k+1} - A x_k - B u_k. \quad (38)$$

This equation is used to estimate v_k from recorded data during a tracking task as previously described. To avoid overfitting, a different sine trajectory with a frequency of 0.22 Hz is used. We approximate the covariance Q by the computed sample covariance of obtained time series data for v_k ,

$$Q = \begin{bmatrix} 4.82 \times 10^{-10} & 8.37 \times 10^{-9} \\ 8.37 \times 10^{-9} & 5.64 \times 10^{-6} \end{bmatrix}. \quad (39)$$

To avoid accuracy problems, we rely on the library [24], which allows for numeric resolution with arbitrary floating-point precision.

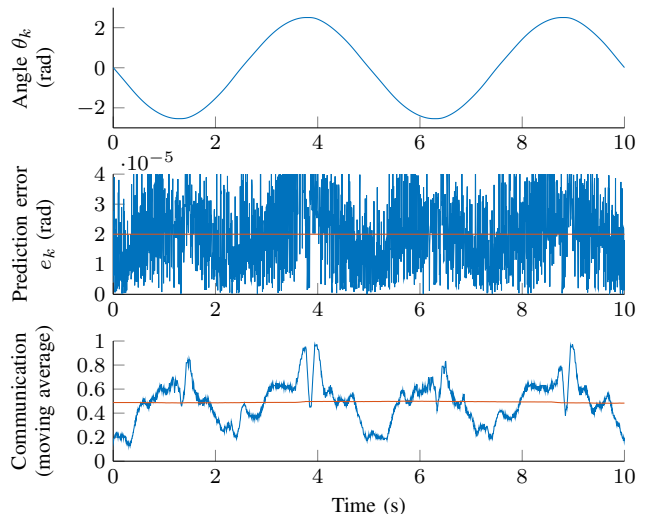


Fig. 3. Event-based estimation for one-link robot experiment with $\delta = 2 \times 10^{-5}$. TOP: angular position. MIDDLE: Triggering signal (6) (blue) and threshold δ (orange). BOTTOM: Communication rate computed as moving horizon average with windows of 0.01 s (blue) and πf (orange).

C. Results

We implement the event-based estimation architecture from Sec. II in order to estimate the state $(\theta_k, \dot{\theta}_k)$ from the encoder measurements during a trajectory tracking experiment. Again, we perform sine tracking with a slightly altered frequency of 0.20 Hz . Corresponding to the remote estimation architecture in Fig. 1, the estimates are not used in feedback and the input torque τ_k is available for both estimation and prediction. For an experiment with trigger threshold $\delta = 2 \times 10^{-5}$, the resulting trajectories of the position θ_k , the triggering signal (6), and the communication rate are shown in Fig. 3. As can be seen from the communication rate computed with a small averaging window (bottom, blue), the communication rate does not converge to a steady-state value in this experiment. Instead, it exhibits the same periodicity as the angle trajectory, which alludes to non-stationary conditions and, in particular, position dependent system properties such as nonlinear friction. For a larger window of half a signal period (orange), however, the position dependent irregularities mostly average out.

Table I shows the empirical communication rates when averaged over the length of the experiment (15s), for the experiment in Fig. 3, as well as other choices of δ (1st column). The empirical rates are compared to the steady-state expected communication rates $\bar{\gamma}$ obtained from the analytical results in Sec. V. In particular, the 0th-order approximation (34) (4th column), and a 9th-order approximation according to Sec. V-D (3rd column) are shown. Note that for $\delta = 4 \times 10^{-5}$, the 0th-order approximation could not be computed since Assumption 3 is not satisfied, and the series in (33) diverges. Despite Assumption 3 not being satisfied, we still applied the higher order approximation, which gave reasonable results.

From the results in Table I, it can be seen that the communication rate decreases when increasing the threshold

TABLE I

EXPERIMENTAL AND ANALYTIC COMMUNICATION RATES

δ	Experimental result	9th order	0th order
1×10^{-5}	69.6%	66.5%	64.9%
2×10^{-5}	49.5%	41.8%	31.3%
3×10^{-5}	36.2%	28.1%	10.1%
4×10^{-5}	27.6%	19.8%	–

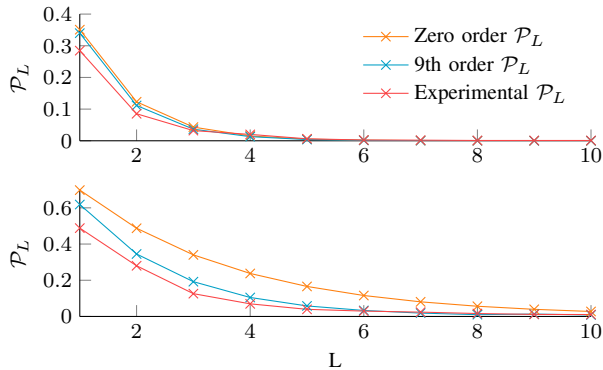


Fig. 4. Comparison of the probability \mathcal{P}_L from 0th- and 9th-order approximations with experimental data (red), for $\delta = 1 \times 10^{-5}$ (top) and $\delta = 2 \times 10^{-5}$ (bottom).

δ , as expected. Furthermore, the quality of the approximation decreases with increasing δ (cf. discussion in Sec. V-D). Generally, the analytic rates are good approximations of the empirical ones, despite Assumption 1 not being satisfied. Presumably, this is because of the averaging effect over multiple periods as discussed above.

The probabilities \mathcal{P}_L (18) are essential for the analytic computation of $\bar{\gamma}$. Figure 4 compares \mathcal{P}_L obtained from the 0th- and 9th-order approximations with the empirical results obtained from the experiment.

VII. CONCLUSION

In this paper, we computed the expected communication rate in a typical event-based state estimation scenario for a linear Gaussian process model. The derived expressions for the transient and steady-state rates are validated against experiments on a one-link robot arm.

While we assumed convergence to steady-state communication rates in the theoretical analysis, the robot experiments displayed rates correlated with the periodic trajectory. When considering the communication rate averaged over one period, however, we found the theoretical results to match well with the empirical ones. Extending the theoretical analysis to this case is an interesting task for future work.

In Sec. V-D, a general approximation of the communication rate involving higher order terms was presented. Both errors induced by using finite M (terms in the summation \mathcal{S}) and finite N (terms in the Taylor series of the exponential) can in principle be bounded using standard techniques. Rigorous derivation of an error bound as a function of M and N is another task for future work.

REFERENCES

- [1] M. Lemmon, "Event-triggered feedback in control, estimation, and optimization," in *Networked Control Systems*. Springer, 2010, pp. 293–358.
- [2] C. G. Cassandras, "The event-driven paradigm for control, communication and optimization," *Journal of Control and Decision*, vol. 1, no. 1, pp. 3–17, 2014.
- [3] M. Miskowicz, *Event-Based Control and Signal Processing*. CRC Press, 2016.
- [4] M. Mazo Jr and P. Tabuada, "Decentralized event-triggered control over wireless sensor/actuator networks," *IEEE Transactions on Automatic Control*, vol. 56, no. 10, pp. 2456–2461, 2011.
- [5] J. Sijs, L. Kester, and B. Noack, "A study on event triggering criteria for estimation," in *17th International Conference on Information Fusion*, July 2014, pp. 1–8.
- [6] C.-F. Lindberg and A. J. Isaksson, "Comparison of different sampling schemes for wireless control subject to packet losses," in *Int. Conf. on Event-Based Control, Communication, and Signal Processing*, Jun. 2015.
- [7] S. Trimpe and M. Campi, "On the choice of the event trigger in event-based estimation," in *Int. Conf. on Event-based Control, Communication, and Signal Processing*, Jun. 2015.
- [8] D. Lehmann and J. Lunze, "Extension and experimental evaluation of an event-based state-feedback approach," *Control Engineering Practice*, vol. 19, no. 2, pp. 101–112, 2011.
- [9] S. Trimpe and R. D'Andrea, "An experimental demonstration of a distributed and event-based state estimation algorithm," in *18th IFAC World Congress*, Aug. 2011, pp. 8811–8818.
- [10] J. Araújo, M. Mazo Jr, A. Anta, P. Tabuada, and K. H. Johansson, "System architectures, protocols and algorithms for aperiodic wireless control systems," *IEEE Transactions on Industrial Informatics*, vol. 10, no. 1, pp. 175–184, Feb 2014.
- [11] S. Trimpe and J. Buchli, "Event-based estimation and control for remote robot operation with reduced communication," in *IEEE International Conference on Robotics and Automation*, May 2015, pp. 5018–5025.
- [12] J. Sijs, B. Noack, M. Lazar, and U. D. Hanebeck, "Time-periodic state estimation with event-based measurement updates," in *Event-Based Control and Signal Processing*. CRC Press, 2016.
- [13] S. Trimpe, "Distributed event-based state estimation," *arXiv preprint*, 2015. [Online]. Available: <http://arxiv.org/abs/1511.05223>
- [14] J. Wu, Q.-S. Jia, K. H. Johansson, and L. Shi, "Event-based sensor data scheduling: Trade-off between communication rate and estimation quality," *IEEE Transactions on Automatic Control*, vol. 58, no. 4, pp. 1041–1046, 2013.
- [15] D. Shi, T. Chen, and L. Shi, "Event-based state estimation of linear dynamical systems: Communication rate analysis," in *American Control Conference*, 2014, pp. 4665–4670.
- [16] D. Han, Y. Mo, J. Wu, S. Weerakkody, B. Sinopoli, and L. Shi, "Stochastic event-triggered sensor schedule for remote state estimation," *IEEE Transactions on Automatic Control*, vol. 60, no. 10, pp. 2661–2675, 2015.
- [17] T. Henningson, "Event-based control and estimation with stochastic disturbances," Ph.D. dissertation, Lund University, Nov. 2008.
- [18] J. Sijs and M. Lazar, "Event based state estimation with time synchronous updates," *IEEE Transactions on Automatic Control*, vol. 57, no. 10, pp. 2650–2655, Oct 2012.
- [19] D. Simon, *Optimal State Estimation: Kalman, H Infinity, and Nonlinear Approaches*. Wiley-Interscience, 2006.
- [20] B. Anderson and J. Moore, *Optimal Filtering*. Englewood Cliffs, NJ: Prentice-Hall, 1979.
- [21] D. Lindley, *Introduction to Probability and Statistics from a Bayesian Viewpoint, Part 1, Probability*. Cambridge University Press, 1965.
- [22] T. Hahn, "Cuba—a library for multidimensional numerical integration," *Computer Physics Communications*, vol. 168, no. 2, pp. 78–95, 2005.
- [23] S. Ebner and S. Trimpe, "Supplemental material for 'Communication Rate Analysis for Event-based State Estimation'," Max Planck Institute for Intelligent Systems, Tech. Rep., 2016. [Online]. Available: <https://am.is.tuebingen.mpg.de/publications/ebner16techrep>
- [24] J. Maddock and C. Kormanyos, "Boost multiprecision," 2016, http://www.boost.org/doc/libs/1_56_0/libs/multiprecision/doc/html/.